Ca^{2+} Dynamics in a Pollen Grain and Papilla Cell during Pollination of Arabidopsis[1]

Megumi Iwano*, Hiroshi Shiba, Teruhiko Miwa, Fang-Sik Che, Seiji Takayama, Takeharu Nagai, Atsushi Miyawaki, and Akira Isogai

Graduate School of Biological Sciences, Nara Institute of Science and Technology, Ikoma, Nara 630–0101, Japan (M.I., H.S., T.M., F.-S.C., S.T., A.I.); and The Institute of Physical and Chemical Research, Wako, Saitama 351–0198, Japan (T.N., A.M.)

Ca^{2+} dynamics in the growing pollen tube have been well documented in vitro using germination assays and Ca^{2+} imaging techniques. However, very few in vivo studies of Ca^{2+} in the pollen grain and papilla cell during pollination have been performed. We expressed yellow cameleon, a Ca^{2+} indicator based on green fluorescent protein, in the pollen grains and papilla cells of Arabidopsis (*Arabidopsis thaliana*) and monitored Ca^{2+} dynamics during pollination. In the pollen grain, $[Ca^{2+}]_{cyt}$ increased at the potential germination site soon after hydration and remained augmented until germination. As in previous in vitro germination studies, $[Ca^{2+}]_{cyt}$ oscillations were observed in the tip region of the growing pollen tube, but the oscillation frequency was faster and $[Ca^{2+}]_{cyt}$ was higher than had been observed in vitro. In the pollinated papilla cell, remarkable increases in $[Ca^{2+}]_{cyt}$ occurred three times in succession, just under the site of pollen-grain attachment. $[Ca^{2+}]_{cyt}$ increased first soon after pollen hydration, with a second increase occurring after pollen protrusion. The third and most remarkable $[Ca^{2+}]_{cyt}$ increase took place when the pollen tube penetrated into the papilla cell wall.

Flowering plant reproduction comprises several sequential steps from pollination to fertilization. In Brassicaceae, a compatible pollen grain adheres to and hydrates on a papilla cell of the stigma. The hydrated pollen germinates and produces a pollen tube that penetrates into the papilla cell wall and then enters the transmitting tissue of the style. Finally, sperm cells inside the pollen tube encounter egg cells, and fertilization occurs.

In vitro pollen germination requires the presence of Ca^{2+}, boron, and an osmoticant such as Suc (Brewbaker and Kwack, 1963). Lack of Ca^{2+} in the growth medium results in morphological abnormalities such as coiling and tip swelling (Shivanna and Rangaswamy, 1992; Taylor and Hepler, 1997). In vitro germination assays using microinjection of a Ca^{2+}-sensitive fluorescent probe revealed a $[Ca^{2+}]_{cyt}$ gradient in the tip of the growing pollen tube (Rathore et al., 1991; Franklin-Tong et al., 1993; Malho et al., 1994; Pierson et al., 1994, 1996). Furthermore, it has been shown that such a tip-localized intracellular $[Ca^{2+}]_{cyt}$ gradient, which arises from the influx of Ca^{2+} at the tube tip, is essential for pollen tube elongation (Franklin-Tong et al., 1993; Malho et al., 1994; Pierson et al., 1994, 1996; Holdaway-Clarke et al., 1997; Messerli and Robinson, 1997; Messerli et al., 2000; Feijo et al., 2001; Plieth, 2001; Robinson and Messerli, 2002; Holdaway-Clarke and Hepler, 2003). These in vitro observations suggest that Ca^{2+} dynamics are involved in the pollination process in vivo. However, because of the difficulty in microinjecting a Ca^{2+}-sensitive probe into an exine-covered pollen grain, such investigations have not been performed. In addition, there have been few reports concerning Ca^{2+} dynamics in papilla cells, because the physical damage caused by microinjection has been shown to perturb the normal pollination process (Dearnaley et al., 1997). Another approach for real-time imaging of Ca^{2+} involves the expression in plant cells of aequorin, a Ca^{2+}-sensitive luminescent protein (Knight et al., 1991). This method, however, requires the incorporation of the cofactor coelenterazine for light emission, and the luminescence is relatively weak. To examine Ca^{2+} dynamics in the pollen grain and papilla cell during pollination, it is important to develop a new, highly sensitive system to monitor real-time Ca^{2+} dynamics in these cells without damaging them.

Yellow cameleons, which are new Ca^{2+} indicators, have been developed to combine the advantages of molecular targeting with a fluorescent readout (Miyawaki et al., 1997, 1999). These indicators are chimeric proteins consisting of an enhanced cyan fluorescent

[1] This work was supported in part by a Grant-in-Aid Creative Scientific Research (grant no. 16GS0316, to A. I.) from Japan Society for the Promotion of Science (JSPS), by a Grant-in-Aid for Special Research (C, grant no. 13640649, to M. I.) from the Ministry of Education, Culture, Sports, Science and Technology of Japan (MEXT), and by the 21st Century Centers of Excellence (COE) Program to Nara Institute of Science and Technology from MEXT.

* Corresponding author; e-mail m-iwano@bs.naist.jp; fax 81–743–72–5459.

Article, publication date, and citation information can be found at www.plantphysiol.org/cgi/doi/10.1104/pp.104.046961.

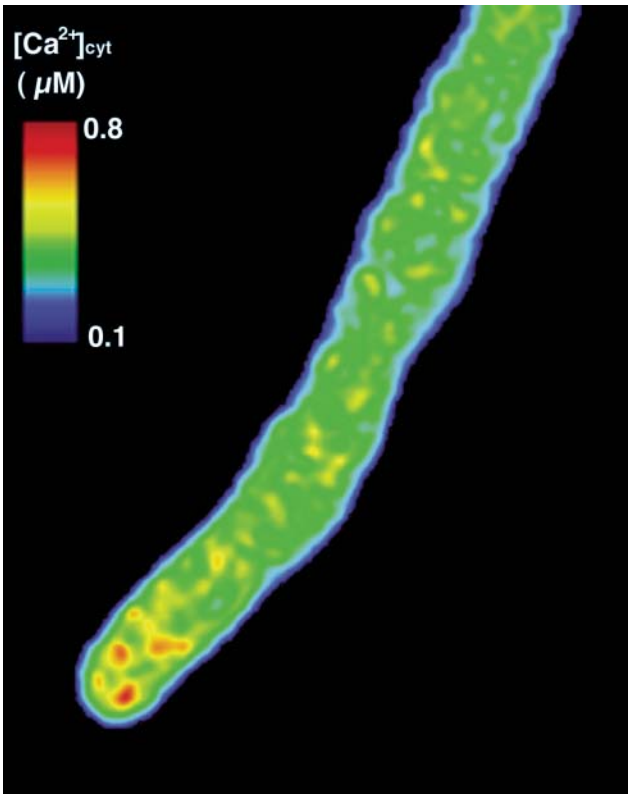

Figure 1. An EYFP:ECFP ratiometric image of the growing pollen tube. ECFP and EYFP images were separated from the total YC3.1 fluorescence image using their individual spectra, and an image depicting their ratio was obtained.

protein (ECFP), calmodulin (CaM), a glycyl-Gly linker, the CaM-binding domain of myosin light chain kinase (M13), and an enhanced yellow fluorescent protein (EYFP). When Ca^{2+} binds to the CaM domain, this domain associates with the M13 peptide, causing the protein to adopt a more compact conformation, which increases the efficiency of fluorescence resonance energy transfer between ECFP and EYFP. Several types of cameleons have been developed with differing affinities for Ca^{2+} due to tunable binding of the CaM domain. Yellow cameleon 2.1 (YC2.1) is a high-affinity indicator and has been shown to be effective in monitoring $[Ca^{2+}]_{cyt}$ in Arabidopsis (*Arabidopsis thaliana*) guard cells (Allen et al., 1999, 2000, 2001). Yellow cameleon 3.1 (YC3.1) is a low-affinity indicator suitable for monitoring rapid changes in $[Ca^{2+}]_{cyt}$ such as those that occur in the pollen tube.

To investigate Ca^{2+} dynamics during pollination, we genetically transformed Arabidopsis to express the *YC3.1* gene in pollen grains and papilla cells. We compared Ca^{2+} dynamics in pollen grains and pollen tubes germinated using in vitro, in vivo, and semi in vivo systems. We also monitored Ca^{2+} dynamics in papilla cells during pollination. These results will be discussed in relation to the physiological relevance of Ca^{2+} dynamics in the pollination process.

RESULTS

Expression of YC3.1 in the Pollen Grains and Ca^{2+} Dynamics in Pollen Germination and Pollen Tube Growth in Vitro

We independently transformed 13 plants with pAct1YC3.1. After selection on kanamycin-containing Murashige and Skoog plates, we confirmed by reverse transcription-PCR that all of the plants were transcribing the transgene. To select the plant with the brightest fluorescence, pollen tubes growing on the germination medium were observed using fluorescence microscopy (Blue excitation, No. 10 filter, Axiophoto; Carl Zeiss, Jena, Germany).

To confirm that green fluorescence was due to the ECFP and EYFP of the genetically expressed YC3.1, we obtained the fluorescence spectra of the growing pollen tubes using a spectral-imaging microscope system with excitation at 458 nm. The YC3.1 spectrum comprised both spectra typically observed from recombinant ECFP and EYFP proteins. Photobleaching with 514-nm light in a 5 μm $\times$ 10-μm area of the pollen tube tip induced an increase in ECFP fluorescence of about 15% and a decrease in EYFP fluorescence (data not shown). This demonstrated that full-length YC3.1 was expressed in the transgenic pollen tubes and that fluorescence resonance energy transfer (FRET) occurred between ECFP and EYFP. To investigate $[Ca^{2+}]_{cyt}$ distribution in the pollen tube, the ECFP and EYFP components of the YC3.1 fluorescence spectra were separated and the EYFP:ECFP ratio was calculated. After digital low-pass filter treatment, the gray-level value of each pixel was expressed with a pseudo-color as shown in Figure 1. Corroborating a previous report, $[Ca^{2+}]_{cyt}$ was found to be higher at the tip region. To investigate Ca^{2+} dynamics at the pollen tube tip, fluorescence images were acquired at 1.2- to 6-s intervals in the 463- to 543-nm range. These images were separated into ECFP and EYFP images. We measured the ECFP and EYFP fluorescence inten-

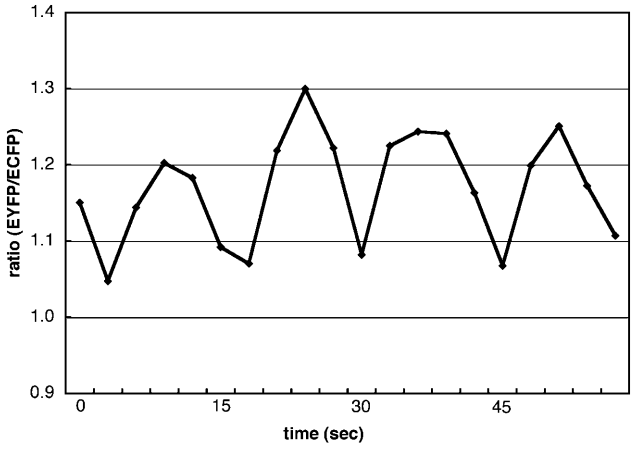

Figure 2. Periodic change of the EYGP:ECFP ratio in a 5 $\times$ 5 μm^2 region of the growing pollen-tube tip observed during in vitro pollination.

Table I. *$[Ca^{2+}]_{cyt}$ oscillation and the growth rate of the growing pollen tube*

Experiment	Oscillation Period	$[Ca^{2+}]_{cyt}$			Mean Growth Rate	No. of Experiment
		Max.	Min.	Mean		
	sec		*μM*[a]		*μm/min*[b]	
In vitro[c]	12 ~ 21	0.68	0.15	0.39	0.7 ± 0.2	16
In vivo	~ 6	1.14	0.64	0.86	13.2 ± 0.3	20
Semi in vivo	9 ~15	2.18	0.91	1.42	2.3 ± 0.2	20

[a]$[Ca^{2+}]_{cyt}$ at the tip region ($5 \times 5\ \mu m^2$) was calculated. Mean values indicate average over time in the individual pollen tubes in all experiments. Max and min values indicate peak and tough values. [b]All values reported as mean ± SD. [c]The growing pollen tube just after germination was monitored.

sities in a 5×5-μm^2 region at the tip and calculated the EYFP:ECFP ratio. At the tip, the value of this ratio oscillated periodically around a mean value of 1.32 ± 0.24 ($n = 16$; Fig. 2). Furthermore, we converted the YC3.1 ratios into approximate $[Ca^{2+}]_{cyt}$ according to the previous report (Allen et al., 1999), and then we estimated that $[Ca^{2+}]_{cyt}$ at the tip region ranged from 0.15 to 0.68 μM and changed periodically with a period between 12 and 21 s (Table I).

To examine Ca^{2+} dynamics during in vitro germination, pollen grains from freshly dehisced anthers were cultured in agar-containing germination medium. Every pollen grain immediately hydrated. The ratiometric images showed that $[Ca^{2+}]_{cyt}$ was distributed almost uniformly throughout the recently hydrated pollen grains (Fig. 3a). One hour after culture, 20% of the pollen grains had protrusions at the potential germination site, and after 2 h about one-half of these pollen grains germinated. In these grains, $[Ca^{2+}]_{cyt}$ was increased at the potential germination site (arrow, Fig. 3b). In many instances, this increase was not exclusive to the germination site but was observed elsewhere in the pollen grain (arrowhead, Fig. 3b). When no $[Ca^{2+}]_{cyt}$ gradient was established in the pollen grain, no protrusion was formed following hydration, and germination did not occur. Furthermore, to examine the relationship between the $[Ca^{2+}]_{cyt}$ gradient and pollen germination, we examined the effect of nifedipine, which blocks L-type Ca^{2+} channels (Dierkes et al., 2004) and inhibits pollen germination. Addition of nifedipine to the germination medium resulted in an almost complete loss of pollen-grain germination. Overall $[Ca^{2+}]_{cyt}$ in treated pollen grains was lower than in untreated ones, and the gradient was never observed (Fig. 3c). These results suggest that a $[Ca^{2+}]_{cyt}$ gradient is required for pollen grain germination.

Ca^{2+} Dynamics in the Pollen Grain and Pollen Tube during in Vivo Pollination

To examine Ca^{2+} dynamics in a pollen grain during pollination, YC3.1 fluorescence was monitored at 1.2- to 30-s intervals after a pollen grain from a pAct1YC3.1-expressing plant was pollinated onto a papilla cell under micromanipulation. During pollination, the YC3.1 fluorescence in the pollen grain and pollen tube were captured and split into ECFP, EYFP, and autofluorescence images. Figure 4 shows a time course of ratiometric images.

Light microscopy revealed the hydration and protrusion of the pollen grain at the site of attachment with the papilla cell 5 min after pollination. Within 20 min, a pollen tube germinated at the site of attachment with the papilla cell, and within 30 min, the pollen tube penetrated the papilla cell wall. Just after pollination, $[Ca^{2+}]_{cyt}$ was high in the central area of the pollen grain (0′00″–2′30″ in Fig. 4). Immediately after hydration, $[Ca^{2+}]_{cyt}$ was evenly distributed (3′00″–9′00″ in Fig. 4). However, before pollen-tube germination, $[Ca^{2+}]_{cyt}$ increased at the potential germination site, where a protrusion signifying imminent germination then appeared (9′30″–15′30″ in Fig. 4). Conversely, when a pollen grain failed to form, such

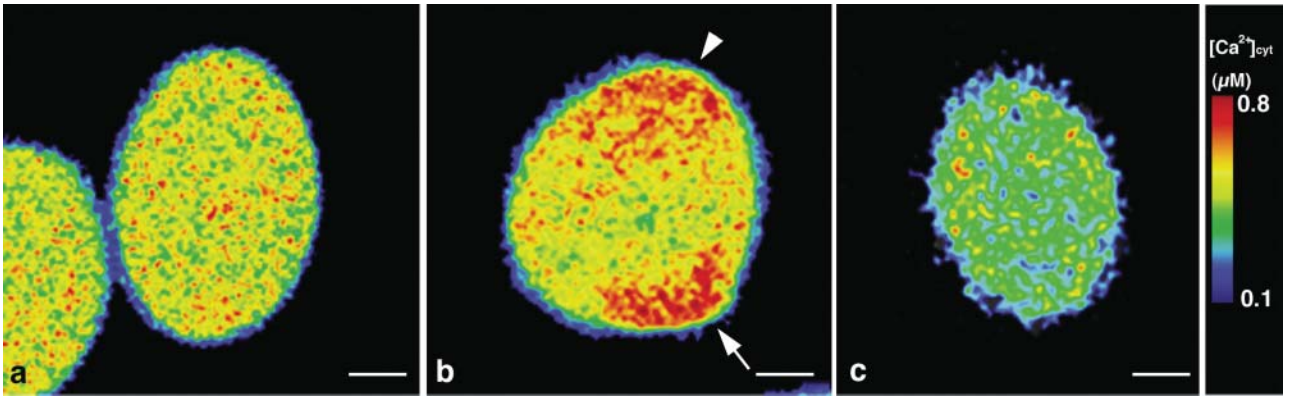

Figure 3. Distribution of Ca^{2+} in the pollen grain during in vitro germination. a, A ratiometric image of the pollen grain after hydration. b, A ratiometric image of a protrusion on a pollen grain. $[Ca^{2+}]_{cyt}$ increase was observed not only at the potential germination site (arrow) but also at another site (arrowhead). c, A ratiometric image of a nifedipine-treated pollen grain after hydration.

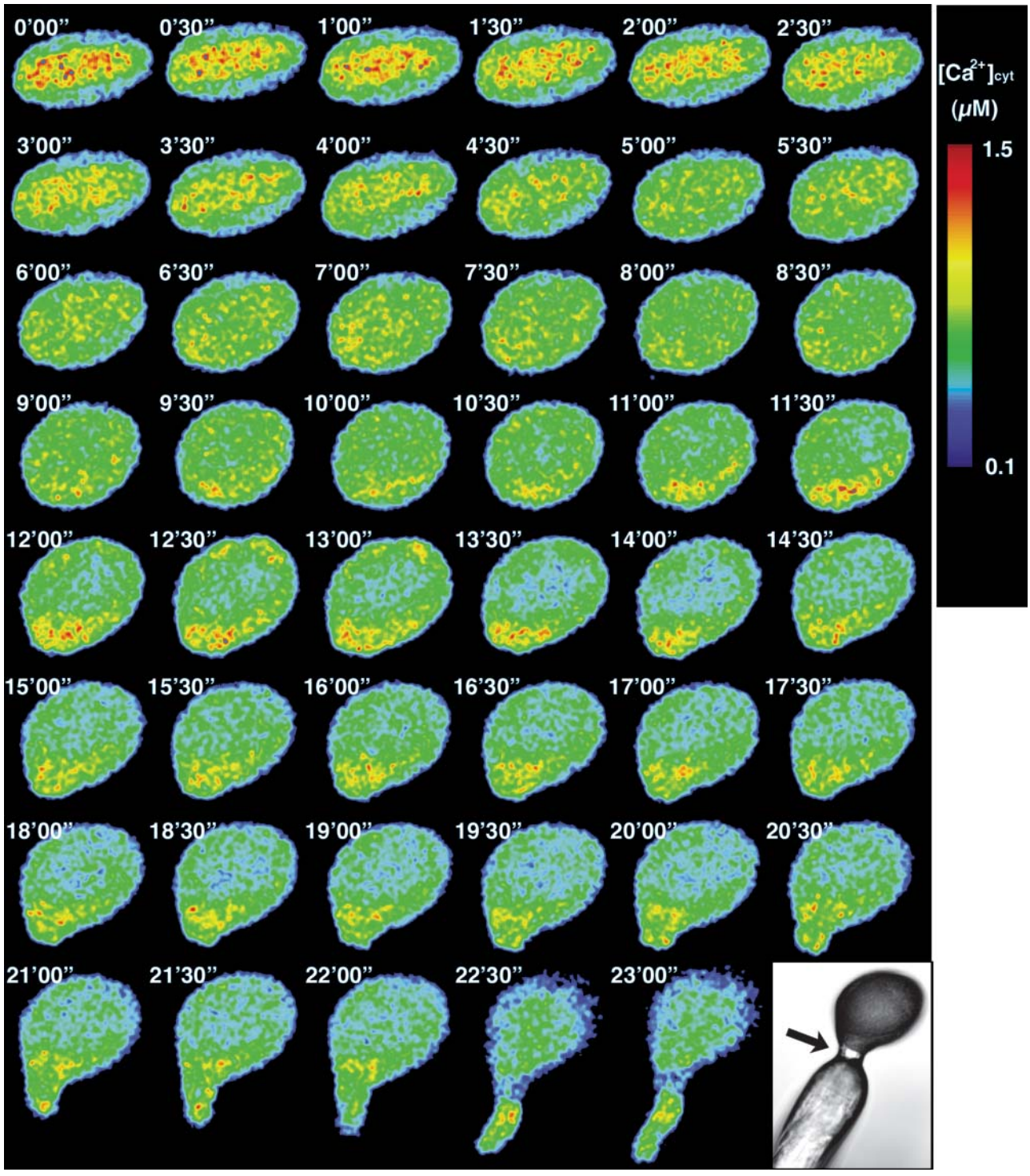

Figure 4. Ca^{2+} dynamics in the pollen grain during in vivo pollination. Monitoring was performed under dry conditions. $[Ca^{2+}]_{cyt}$ was high at the center of the pollen grain before hydration. $[Ca^{2+}]_{cyt}$ was increased at the potential germination site during hydration (9′30″–15′30″). The accumulation continued until germination (approximately 22′30″).

a localized increase in $[Ca^{2+}]_{cyt}$, pollen tube germination did not occur (data not shown). These results demonstrate that an increase in $[Ca^{2+}]_{cyt}$ at the potential germination site precedes pollen germination in vivo as well as in vitro.

During the period from germination to penetration of the papilla cell wall, $[Ca^{2+}]_{cyt}$ changed frequently at the tip of the pollen tube. Furthermore, when the pollen tube elongated within the papilla cell after penetration, changes in $[Ca^{2+}]_{cyt}$ were observed not

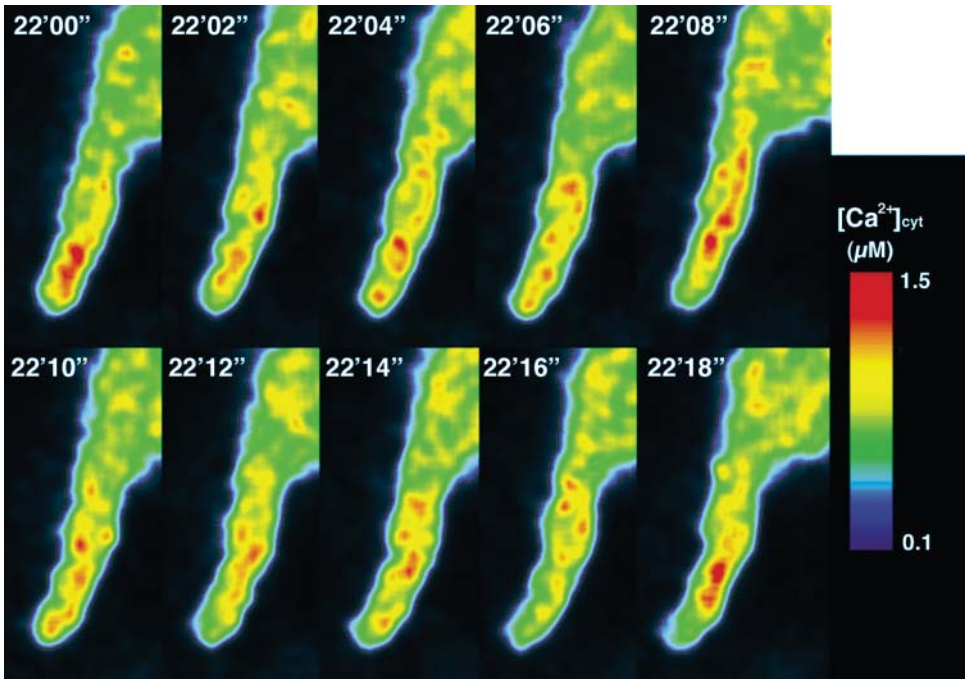

Figure 5. Ca^{2+} dynamics during the elongation of a pollen tube in the papilla cell wall. In the growing pollen tube, frequent changes of $[Ca^{2+}]_{cyt}$ throughout the tube were observed.

only at the tip, but also throughout the elongated pollen tube (Fig. 5). The mean value of the ratio at the tube tip was 1.69 ± 0.16 (n = 20), representing a mean $[Ca^{2+}]_{cyt}$ of 0.86 μM (range, 0.64–1.14 μM; Table I). The period of the $[Ca^{2+}]_{cyt}$ oscillation was shorter (3.6–6 s; Fig. 6) than that observed in vitro, although a faster monitoring system with higher resolution, such as a cooled charged coupled device (CCD) camera, would be required to determine the oscillation period more precisely. The $[Ca^{2+}]_{cyt}$ near the penetration site, however, was frequently elevated (Fig. 7). At this site, the pollen tube changed its direction of elongation.

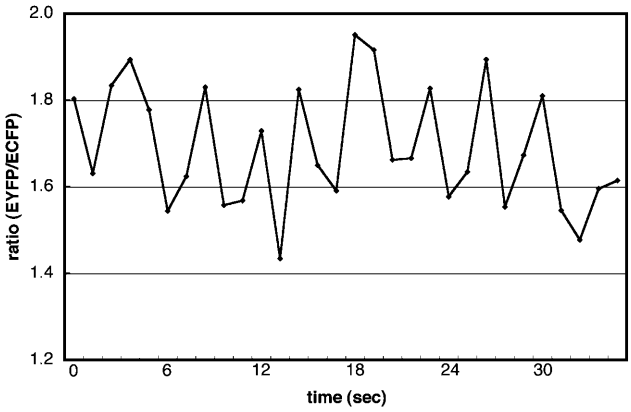

Figure 6. Periodic changes in the EYGP:ECFP ratio in a 5 × 5 μm^2 region at the tip of the growing pollen tube within the papilla cell wall observed during in vivo pollination.

Ca^{2+} Dynamics in a Semi in Vivo Growing Pollen Tube

As demonstrated by the observed changes in $[Ca^{2+}]_{cyt}$, the $[Ca^{2+}]_{cyt}$ oscillation period in the pollen grain was shorter in vivo than in vitro. Therefore, we speculated that molecules from the papilla cell affect $[Ca^{2+}]_{cyt}$ distribution in the pollen tube. To study whether Ca^{2+} dynamics in a pollen tube passing through the pistil are different from those in vitro, we monitored $[Ca^{2+}]_{cyt}$ in the growing pollen tube under semi in vivo conditions. Figure 8 shows the tip of the growing pollen tube at 3-s intervals. The mean value of the EYFP:ECFP fluorescence ratio at the tip was 1.98 ± 0.26 (n = 20), representing a mean $[Ca^{2+}]_{cyt}$ of 1.42 μM (range, 0.91–2.18 μM; Table I), which was higher than that observed in vitro. The oscillation period varied between 9 and 15 s (Fig. 9).

Ca^{2+} Dynamics in the Papilla Cell during in Vivo Pollination

The in vitro, nifedipine-induced inhibition of $[Ca^{2+}]_{cyt}$ increase and pollen germination suggested that the Ca^{2+} required for pollen germination is internalized from the external medium. We hypothesized, then, that Ca^{2+} in the papilla cell would affect germination in vivo. To examine Ca^{2+} dynamics in the papilla cell during pollination, a construct encoding the *YC3.1* gene driven by the *SLG* promoter, which is highly expressed in the stigma of Brassica, was transformed into Arabidopsis. We obtained five transgenic plants and selected the plant with the brightest YC3.1 fluorescence.

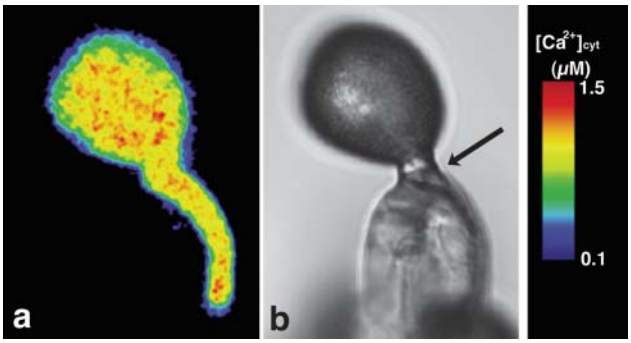

Figure 7. Ca^{2+} distribution in the elongated pollen tube within the papilla cell wall. This image was constructed from a series of optical sections taken at 1.0-μm intervals. An increase in $[Ca^{2+}]_{cyt}$ was observed near the penetration site (an arrow) into the papilla cell.

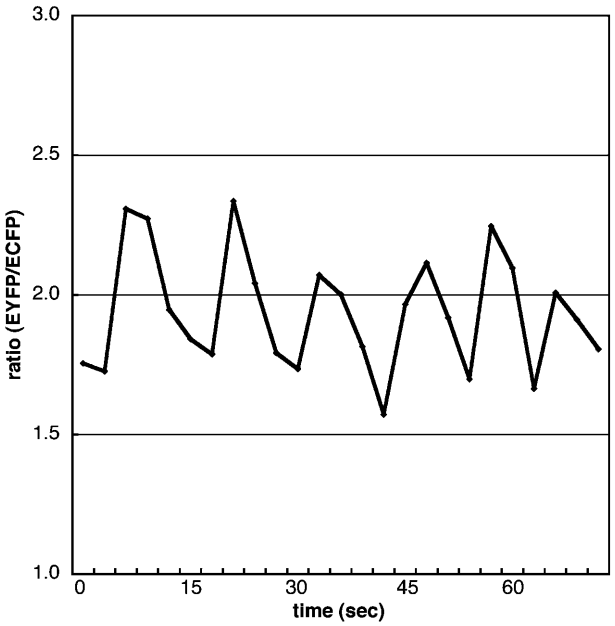

Figure 9. Periodic changes in the EYGP:ECFP ratio in a 5 × 5-μm^2 region at the tip of the growing pollen tube under semi in vivo conditions.

Before pollination, no local increase of $[Ca^{2+}]_{cyt}$ was observed (before, Fig. 10). $[Ca^{2+}]_{cyt}$ near the surface was estimated to be below 0.1 μM. During pollination, however, remarkable $[Ca^{2+}]_{cyt}$ increases in the papilla cell directly apposing the pollen grain occurred several times (Fig. 10). Later in the hydration period (6′00″ in Fig. 10), increases in $[Ca^{2+}]_{cyt}$ near the pollen attachment site were prominent. During this hydration period, $[Ca^{2+}]_{cyt}$ in the pollen grain increased at the potential germination site (Fig. 4). Before pollen germination (9′00″ and 10′00″ in Fig. 10), $[Ca^{2+}]_{cyt}$ was increased locally near the pollen attachment site, and in the pollen grain itself, $[Ca^{2+}]_{cyt}$ was highest at the tip and decreased from there (Fig. 4). Furthermore, before penetration of the pollen tube into the papilla cell (12′00″ in Fig. 10), $[Ca^{2+}]_{cyt}$ increased at the site of pollen tube attachment. The increase in $[Ca^{2+}]_{cyt}$ continued during the elongation of the pollen tube. The maximum $[Ca^{2+}]_{cyt}$ after pollination was estimated to be 0.8 μM. We observed a similar increase in $[Ca^{2+}]_{cyt}$ during in vivo pollination in 20 independent experiments. These observations indicate that the increase in $[Ca^{2+}]_{cyt}$ in the papilla cell is induced by pollination and that interaction between a pollen grain and a papilla cell during pollination is mediated through Ca^{2+}.

Growth Rate

We examined the mean growth rates of the growing pollen tubes using in vitro, in vivo, and semi in vivo techniques (Table I). The mean growth rate was fastest in vivo and slowest in vitro. Thus, the growth rate was

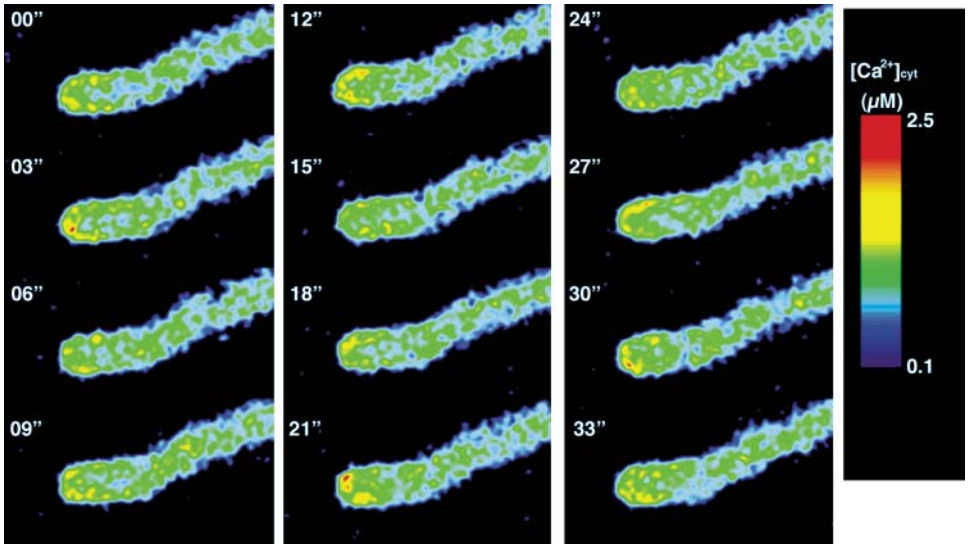

Figure 8. Ca^{2+} distribution in the growing pollen tube under semi in vivo conditions. Periodic changes in $[Ca^{2+}]_{cyt}$ were observed at the tube's tip.

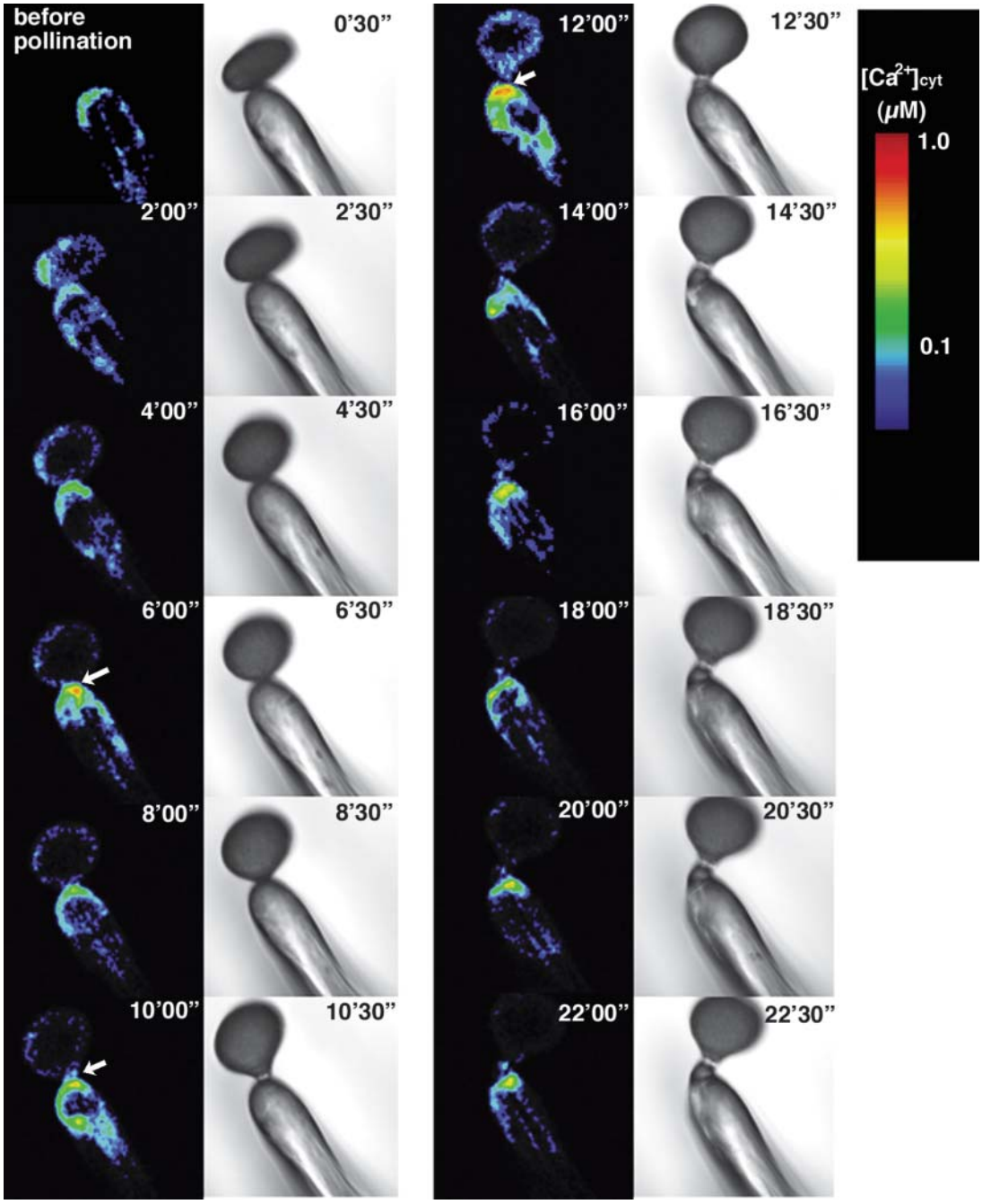

Figure 10. Ca^{2+} distribution in the papilla cell during pollination. Arrows represent notable increases in $[Ca^{2+}]_{cyt}$, which were typically observed 6, 10, and 12 min after pollination.

inversely proportional to the period of $[Ca^{2+}]_{cyt}$ oscillation at the tip of the pollen tube.

DISCUSSION

Using transgenic Arabidopsis expressing YC3.1, we have analyzed here for the first time, to our knowledge, the Ca^{2+} dynamics of a single pollen grain and a papilla cell during pollination. In the pollen grain, $[Ca^{2+}]_{cyt}$ was increased at the potential germination site after hydration, and a tip-focused gradient of $[Ca^{2+}]_{cyt}$ was formed before germination. After penetration into the papilla cell wall, rapid oscillation of $[Ca^{2+}]_{cyt}$ was observed at the tip of the growing pollen tube. In the papilla cell, on the other hand, $[Ca^{2+}]_{cyt}$ increased periodically during pollen hydration, after pollen protrusion, and during pollen tube penetration. These increases in $[Ca^{2+}]_{cyt}$ in the papilla cell were correlated with the behavior of the attached pollen grain.

In the rehydrated pollen grain, a $[Ca^{2+}]_{cyt}$ gradient was observed before germination both in vivo and in vitro. Treatment with the Ca^{2+} channel blocker nifedipine was shown to inhibit both $[Ca^{2+}]_{cyt}$ gradient formation and pollen germination in vitro. Such inhibition has also been reported in *Narcissus pseudonarcissus* (Heslop-Harrison and Heslop-Harrison, 1992a, 1992b). These results suggest that a pregermination $[Ca^{2+}]_{cyt}$ gradient, presumably formed by Ca^{2+} influx through L-type Ca^{2+} channels, is essential for pollen tube germination. However, the pulsatile growth of the pollen tube in Nicotiana and Petunia has been shown to be sensitive to gadolinium and lanthanum but not to nifedipine (Malho et al., 1995; Geitmann and Cresti, 1998; Feijo et al., 2001; Holdaway-Clarke and Hepler, 2003). Furthermore, in the growing hyphae of fungi, which display similar Ca^{2+} dynamics to the growing pollen tube, stretch-activated channels have been discovered on the plasma membrane, and the apical $[Ca^{2+}]_{cyt}$ gradient can be blocked with gadolinium (Garrill et al., 1992, 1993). Finally, it has been suggested that stretch-activated channels are involved directly in pollen tube growth (Holdaway-Clarke and Hepler, 2003). However, it is not clear whether stretch-activated channels exist in the potential germination site of the pollen grain or whether the same Ca^{2+} channels are used both in establishing the pregermination $[Ca^{2+}]_{cyt}$ gradient and in maintaining the tip of the growing pollen tube. To elucidate this issue, these in vitro effects of selective Ca^{2+} channel blockers on $[Ca^{2+}]_{cyt}$-gradient formation during pollen germination should be examined in vivo using transgenic Arabidopsis expressing YC3.1.

The in vivo-pollinated pollen tube exhibited a higher growth rate than those pollinated under in vitro or semi in vivo conditions. The oscillation frequency of $[Ca^{2+}]_{cyt}$ at the tip was also fastest in the in vivo-pollinated pollen tubes. However, the $[Ca^{2+}]_{cyt}$ level at the tip was intermediate in the in vivo pollination. The elongation rate of a growing neuron has been shown to be correlated with the intracellular calcium level at the growth cone, with maximal outgrowth occurring at an optimal $[Ca^{2+}]_{cyt}$ in the growth cone (Kater and Mills, 1991). By analogy with these results in neurons, $[Ca^{2+}]_{cyt}$ in in vivo-pollinated pollen tubes might be optimal for pollen tube growth. However, these results must be interpreted cautiously due to the wide variety of factors other than Ca^{2+} that presumably affect pollen tube growth.

Under semi in vivo germination conditions, the oscillation frequency of $[Ca^{2+}]_{cyt}$ at the growing pollen tip and the pollen tube's growth rate were both faster than those observed under in vitro conditions. Furthermore, $[Ca^{2+}]_{cyt}$ was higher semi in vivo compared to in vitro. Under semi in vivo conditions, the germination medium contains various substances from the pistil, which modify the growth rate of the pollen tube. In fact, transmitting tissue-specific protein, a substance secreted by the pistil, has been shown in tobacco to attract pollen tubes and stimulate their growth (Cheung et al., 1995). Thus, YC3.1-expressing pollen grains will be useful to search for molecules that mediate $[Ca^{2+}]_{cyt}$ dynamics in the pollen tube.

$[Ca^{2+}]_{cyt}$ in the apical region of the papilla cell was shown to increase from its low level before pollination at the site of pollen grain attachment during pollen hydration. This result suggests that a pollen grain induces a local increase of $[Ca^{2+}]_{cyt}$ in an adjacent papilla cell. In addition, after this local $[Ca^{2+}]_{cyt}$ increase in the papilla cell, a pregermination $[Ca^{2+}]_{cyt}$ gradient formed in the pollinated pollen grain. These results suggest that the $[Ca^{2+}]_{cyt}$ gradient is formed by the influx of Ca^{2+} from the papilla cell, although it is not clear whether the Ca^{2+} comes from the cytoplasm or cell wall of the papilla.

Reproduction in flowering plants comprises several sequential steps, from pollination to fertilization. In this study, we have monitored Ca^{2+} dynamics in the pollen grain, pollen tube, and papilla cell during the early steps of the reproductive process using YC3.1-expresseing Arabidopsis. This novel monitoring system makes possible the detailed study of Ca^{2+} dynamics throughout the reproductive process. Furthermore, this system should be useful for investigating mechanisms by which a pollen tube and style communicate.

MATERIALS AND METHODS

Transgenic Constructs

A cassette containing the YC3.1-coding region followed by the nopaline synthase polyadenylation signal from pBIYC3.1 was constructed by replacing the β-glucuronidase-coding sequence of pBI221 (CLONTECH Laboratories, Palo Alto, CA) with a YC3.1-coding region. The 1.5-kb fragment upstream of the Act1 gene, which is highly expressed in the reproductive tissues (An et al., 1996), was isolated from genomic DNA of a *Brassica rapa* S9 homozygote, and the 2.2-kb fragment upstream of the SLG9 gene, which is highly expressed in the papilla cell (Suzuki et al., 1997a), was obtained from a P1-derived artificial chromosome clone, E89 (Suzuki et al., 1997b). These fragments were reamplified by PCR using specific primers designed to add *Hin*dIII and *Xba*I, and *Sph*I and *Sma*I restriction sites to the 5′ and 3′ ends, respectively, as follows. For amplification of the 5′-flanking region of the Act1 gene: sense primer, 5′-GAAGCTTTCTCTTTAAAAGTTAAGTTTTCTTTGTACATGTCTCTAAGC-3′; and antisense primer, 5′-GTCTAGATTTCTTCTACCTTTATGCAAATCCAAACATTGTTTAAAGATC-3′; for amplification of 5′-flanking region of the SLG9 gene: sense primer, 5′-GGATGCAAAGCATGCATTGAATTATTAGA-3′; and antisense primer, 5′-CCCGGGCTCTCTCCCCACCTTTTTCTTTC-3′. The amplified fragments were subcloned into pBIYC3.1 to yield Act1 promoter-YC3.1 and SLG9 promoter-YC3.1 constructs, respectively. These chimeric genes, comprising the 1.5-kb promoter region of the Act1 gene, the YC3.1 coding sequence, and the nopaline synthase transcription terminator, or the 2.2-kb promoter region of the SLG9 gene, the YC3.1 coding sequence, and the nopaline synthase transcription terminator, were inserted into the binary vector pSLJ1006 (Jones et al., 1992) to create pAct1YC3.1 and pSLG9YC3.1, respectively.

Transformation

pSLJAct1YC3.1 and pSLJSLG9YC3.1 plasmids were electroporated into the *Agrobacterium tumefaciens* strain EHA105 (Hood et al., 1993). The Agrobacterium infiltration procedure was performed on unopened flower buds of Arabidopsis, ecotype Columbia, as previously described (Bechtold et al., 1993). The transformed seeds were selected on 1/2 Murashige and Skoog

plates containing kanamycin (50 μg/mL) and were analyzed by PCR amplification for the presence of YC3.1 genes.

Plant Growth Conditions

Arabidopsis (*Arabidopsis thaliana*) plants, ecotype Columbia, were grown in mixed soil in a growth chamber. The light intensity was 120 to 150 μmol m^{-2} s^{-1} during a 12-h daily light period. The temperature was 22°C ± 2°C.

Fluorescence Imaging

For in vitro imaging, pollen grains from freshly dehisced anthers of YC3.1-expressing plants were mounted on germination medium containing 2 mM $CaCl_2$, 1.65 mM boric acid, 1% (w/v) agar (Ultra-low gelling temperature type IX-A; Sigma, St. Louis), and 17% (w/v) Suc (pH was adjusted with KOH to 7.0; Preuss et al., 1993) in moistened glass-bottomed dishes. After 2 to 6 h at 20°C, $[Ca^{2+}]_{cyt}$ was monitored in pollen tubes growing out of the style using a spectral imaging fluorescence microscope system (LSM510 META, Carl Zeiss). This system is capable of resolving the spectra of fluorescence images; therefore, we could obtain images with no interference between overlapping fluorescence emissions (Haraguchi et al., 2002). Samples were scanned by an argon laser (excitation 458 nm). A Zeiss 63× W.Korr, 1.2 nicotianamine fluorescence objective was used for imaging of pollen tubes and an LD40× Korr, 0.6 nicotianamine fluorescence objective for imaging of papilla cells.

To examine the effect of a Ca^{2+} channel blocker, nifedipine (Sigma, Poole, UK) was dissolved in dimethyl sulfoxide and added to the above germination medium to give a final concentration of 10^{-5} to 10^{-4} M (Heslop-Harrison and Heslop-Harrison, 1992b). Dimethyl sulfoxide alone had no discernible effect on germination and tube growth.

For in vivo imaging, a pistil was mounted on a coverslip prior to pollination and fixed with double-sided tape. After a pollen grain was mounted on a papilla cell using a micromanipulator, $[Ca^{2+}]_{cyt}$ was monitored under dry conditions using the microscope system described above.

For semi in vivo imaging, flowers of wild-type Arabidopsis were excised before dehiscion and attached to an agar plate after the anthers were removed from the flowers. Pollen grains from freshly dehisced anthers of YC3.1-expressing plants were attached to the wild-type stigma. Thirty minutes after pollination, the upper half of the pollinated pistil was excised and mounted on the above germination medium in a moistened glass-bottomed dish. After 2 h incubation at 20°C, $[Ca^{2+}]_{cyt}$ in the pollen tubes growing through the style was monitored using the microscope system described above.

Ratiometric Imaging

Basic ECFP and EYFP spectra were obtained and registered using recombinant CFP-CaM protein and M13-YFP protein expressed in *Escherichia coli* or onion cells that transiently express the 35S promotor-CFP-CaM gene or the 35S promotor-M13-YFP gene. The autofluorescence spectrum for pollen grains was captured and registered using wild plants. After YC3.1 fluorescence was captured in each experiment, the images could be split into ECFP, EYFP, and autofluorescence channels based on the registered spectra. Ratiometric images (EYFP/ECFP) were obtained using image processing software (Laser Lixel, Bio-Rad Laboratories, Hercules, CA).

Calibration of YC3.1 Ratiometric Changes

Calibration of $[Ca^{2+}]_{cyt}$ was carried out as described previously (Allen et al., 1999). Serial dilutions of purified YC3.1 protein were made in Ca^{2+} calibration buffer (Molecular Probes, Eugene, OR), in which free Ca^{2+} concentration ranged from 0 μM to 39 μM. YC3.1 dilutions that gave similar intensities to those seen in YC3.1-expressing pollen tubes were used to determine R_{min} and R_{max}. And values for R_{min} of 0.92 and R_{max} of 3.11 were obtained. These values of R_{min} and R_{max} were used to convert YC3.1 fluorescence ratios into $[Ca^{2+}]_{cyt}$ by fitting them to the YC3.1 in vitro calibration curve (see Miyawaki et al., 1999; Fig. 2B).

Growth Rate

We printed images of EYFP fluorescence in the growing pollen tube and measured the length of the tube using a ruler. The growth rate was calculated from the length of elongation between time points and the interval.

ACKNOWLEDGMENTS

We thank Miss Yamaguchi, Mrs. Onishi, Mrs. Yoneyama, Miss Sugita, and Mrs. Ichikawa for their technical assistance.

Received May 25, 2004; returned for revision August 8, 2004; accepted August 9, 2004.

LITERATURE CITED

Allen GJ, Chu SP, Harrington CL, Schumacher K, Hoffman T, Tang YY, Grill E, Schroeder JI (2001) A defined range of guard cell calcium oscillation parameters encodes stomatal movements. Nature **411:** 1053–1057

Allen GJ, Chu SP, Schumacher K, Shimazaki CT, Vafeados D, Kemper A, Hawke SD, Tallman G, Tsien RY, Harper JF, et al (2000) Alteration of stimulus-specific guard cell calcium oscillations and stomatal closing in Arabidopsis det3 mutant. Science **289:** 2338–2342

Allen GJ, Kwak JM, Chu SP, Llopis J, Tsien RY, Harper JF, Schroeder JI (1999) Cameleon calcium indicator reports cytoplasmic calcium dynamics in Arabidopsis guard cells. Plant J **19:** 735–747

An YQ, Huang S, McDowell JM, McKinney EC, Meagher RB (1996) Conserved expression of the Arabidopsis ACT1 and ACT3 actin subclass in organ primordia and mature pollen. Plant Cell **8:** 15–30

Bechtold N, Ellis J, Pelletier G (1993) In planta Agrobacterium mediated gene transfer by infiltration of adult *Arabidopsis thaliana* plants. C R Acad Sci Paris Life Sci **316:** 1194–1199

Brewbaker JL, Kwack BH (1963) The essential role of calcium ion in pollen germination and pollen tube growth. Am J Bot **50:** 859–865

Cheung AY, Wang H, Wu H-m (1995) A floral transmitting tissue-specific glycoprotein attracts pollen tubes and stimulates their growth. Cell **82:** 383–393

Dearnaley JDW, Levina NN, Lew RR, Heath IB, Goring DR (1997) Interrelationships between cytoplasmic Ca peaks, pollen hydration and plasma membrane conductances during compatible and incompatible pollinations of *Brassica napus* papillae. Plant Cell Physiol **38:** 985–999

Dierkes PW, Wende V, Hochstrate P, Schlue WR (2004) L-type Ca^{2+} channel antagonists block voltage-dependent Ca^{2+} channel in identified leech neurons. Brain Res **1013:** 159–167

Feijo JA, Sainhas J, Holdaway-Clarke T, Cordeiro MS, Kunkel JG, Hepler PK (2001) Cellular oscillations and the regulation of growth: the pollen tube paradigm. Bioessays **23:** 86–94

Franklin-Tong VE, Ride JP, Read ND, Trewavas AJ, Franklin FCH (1993) The self-incompatibility response in *Papaver rhoeas* is mediated by cytosolic free calcium. Plant J **4:** 163–177

Garrill A, Lew RR, Heath IB (1992) Stretch-activated Ca^{2+} and Ca^{2+}-activated K^+ channels in the hyphal tip plasma membrane of oomycete *Saprolegnia ferax*. J. Cell Science **101:** 721–730

Garrill A, Jackson SL, Lew RR, Heath IB (1993) Ion channel activity and tip growth: tip-localized stretch-activated channels generate an essential Ca^{2+} gradient in the oomycete *Saprolegnia ferax*. Eur J Cell Biol **60:** 358–365

Geitmann A, Cresti M (1998) Ca^{2+} channels control the rapid expansions in pulsating growth of Petunia hybrida pollen tubes. J Plant Physiol **152:** 439–447

Haraguchi T, Shimi T, Koujin T, Hashiguchi N, Hiraoka Y (2002) Spectral imaging fluorescence microscopy. Genes Cell **7:** 881–887

Heslop-Harrison J, Heslop-Harrison Y (1992a) Germination of monocolpate angiosperm pollen: evolution of the cytoskelton and wall during hydration, activation and tube emergence. Ann Bot (Lond) **69:** 385–394

Heslop-Harrison J, Heslop-Harrison Y (1992b) Germination of monocolpate angiosperm pollen: effects of inhibitory factors and the Ca^{2+}-channel blocker nifedipine. Ann Bot (Lond) **69:** 395–403

Holdaway-Clarke TL, Feijo JA, Hackett GR, Kunkel JG, Hepler PK (1997) Pollen tube growth and the intracellular cytosolic calcium gradient oscillate in phase while extracellular calcium influx is delayed. Plant Cell **9:** 1999–2010

Holdaway-Clarke TL, Hepler PK (2003) Control of pollen tube growth: role of ion gradients and fluxes. New Phytol **159:** 539–563

Hood EE, Gelvin SB, Melchers LS, Hoekema A (1993) New Agrobacterium helper plasmids for gene transfer to plants. Transgenic Res **2:** 208–218

Jones JDG, Shlumukov L, Carland F, English J, Scofield SR, Bishop GJ, Harrison K (1992) Effective vectors for transformation, expression of heterologous genes, and assaying transposon excision in transgenic plants. Transgenic Res **1:** 285–297

Kater SB, Mills LR (1991) Regulation of growth cone behavior by calcium. J Neurosci **11:** 891–899

Knight MR, Campbell AK, Smith SM, Trewavas AJ (1991) Transgenic plant aequorin reports the effects of touch and cold-shock and elicitors on cytoplasmic calcium. Nature **8:** 524–526

Malho R, Read ND, Pais M, Trewavas AJ (1994) Role of cytosolic calcium in the reorientation of pollen tube growth. Plant J **5:** 331–341

Malho R, Read ND, Trewavas AJ, Pais MS (1995) Calcium channel activity during pollen tube growth and reorientation. Plant Cell **7:** 1173–1184

Messerli M, Robinson KR (1997) Tip localized Ca^{2+} pulses are coincident with peak pulsatile growth rates in pollen tubes of *Lilium logiflorum.* J Cell Sci **110:** 1269–1278

Messerli MA, Creton R, Jaffe LF, Robinson KR (2000) Periodic increases in elongation rate precede increases in cytosolic Ca^{2+} during pollen tube growth. Dev Biol **222:** 84–98

Miyawaki A, Griesbeck O, Tsien RY (1999) Dynamic and quantitative Ca^{2+} measurements using improved cameleons. Proc Natl Acad Sci USA **96:** 2135–2140

Miyawaki A, Llopis J, Heim R, McCaffery JM, Adams JA, Ikura M, Tsien RY (1997) Fluorescent indicators for Ca^{2+} based on green fluorescent proteins and calmodulin. Nature **388:** 834–835

Pierson ES, Miller DD, Callaham DA, Shipley AM, Rivers BA, Cresti M, Hepler PK (1994) Pollen tube growth is coupled to the extracellular calcium ion flux and the intracellular calcium gradient: effect of BAPTA-type buffers and hypertonic media. Plant Cell **6:** 1815–1828

Pierson ES, Miller DD, Callaham DA, van Aken J, Hackett G, Hepler PK (1996) Tip-localized entry fluctuates during pollen tube growth. Dev Biol **174:** 160–173

Plieth C (2001) Plant calcium signaling and monitoring: pros and cons and recent experimental approaches. Protoplasma **218:** 1–23

Preuss D, Lemieux B, Yen G, Davis RW (1993) A conditional sterile mutation eliminates surface components from Arabidopsis pollen and disrupts cell signaling during fertilization. Genes Dev **7:** 974–985

Rathore KS, Cork RJ, Robinson KR (1991) A cytoplasmic gradient of Ca is correlated with the growth of Lily pollen tubes. Dev Biol **148:** 612–619

Robinson KR, Messerli M (2002) Pulsating ion fluxes and growth at the pollen tube tip. Science **162:** 51–53

Shivanna KR, Rangaswamy NS (1992) Pollen Biology. Springer-Verlag, Berlin

Suzuki G, Watanabe M, Isogai A, Hinata K (1997a) Highly conserved 5′-flanking regions of two self-incompatibility genes, *SLG9* and *SRK9*. Gene **191:** 123–126

Suzuki G, Watanabe M, Toriyama K, Isogai A, Hinata K (1997b) Direct cloning of the Brassica S locus by using a P1-derived artificial chromosome (PAC) vector. Gene **199:** 133–137

Taylor LP, Hepler PK (1997) Pollen germination and tube growth. Annu Rev Plant Physiol Plant Mol Biol **48:** 461–491